

07.1;07.2;07.3

## Properties of AlP/Si heterostructure fabricated by combination of plasma enhanced and atomic layer deposition

© A.S. Gudovskikh<sup>1,2</sup>, A.I. Baranov<sup>1</sup>, A.V. Uvarov<sup>1</sup>, E.A. Vyacheslavova<sup>1</sup>, A.A. Maksimova<sup>1,2</sup>,  
E.V. Nikitina<sup>1</sup>, I.P. Soshnikov<sup>1,3,4</sup>

<sup>1</sup> Alferov Federal State Budgetary Institution of Higher Education and Science Saint Petersburg National Research Academic University of the Russian Academy of Sciences, St. Petersburg, Russia

<sup>2</sup> St. Petersburg State Electrotechnical University „LETI“, St. Petersburg, Russia

<sup>3</sup> Ioffe Institute, St. Petersburg, Russia

<sup>4</sup> Institute of Analytical Instrument Making, Russian Academy of Sciences, St. Petersburg, Russia

E-mail: gudovskikh@spbau.ru

Received March 28, 2024

Revised April 12, 2024

Accepted April 22, 2024

For the first time, AlP/Si heterostructures were formed using the method of combined plasma-enhanced and atomic layer deposition and studies of their electronic properties were carried out. Experimentally estimated conduction band offset  $\Delta E_C$  at the AlP/Si interface ( $0.35 \pm 0.10$  eV) is significantly less compared to that of the valence band offset. Thus AlP could be considered as an electron selective contact to Si for solar cells

**Keywords:** aluminum phosphide, silicon, selective contact, solar cell.

DOI: 10.61011/TPL.2024.08.58916.19935

Silicon is the main material for construction of a wide range of semiconductor devices, including high-efficiency solar cells. Heterostructures based on a combination of wide-bandgap materials and silicon may raise significantly the efficiency of photoelectric conversion. A winning combination of band structure and low density of states at the heterointerface translated into record-high efficiency values (26.7%) solar cells based on *a*-Si:H/*c*-Si heterostructures [1]. One way to increase the efficiency further is to reduce the short-wave absorption loss in *a*-Si:H layers by replacing them with wider-bandgap ones. This approach was used successfully in structures with oxide (MoO<sub>3</sub>, WO<sub>3</sub>, and V<sub>2</sub>O<sub>5</sub>) and fluoride (LiF and MgF<sub>2</sub>) layers [2]. However, the possibility of growing lattice-matched materials on a Si surface, which potentially allows one to reduce the density of surface defects acting as recombination centers, is of greater interest. In view of this, it appears necessary to examine the growth of binary compounds GaP and AlP that have a mismatch of 0.4 and 0.5%, respectively. The properties of the heterojunction between GaP (2.26 eV) and Si (1.12 eV) have been studied well. It is known that valence band offset  $\Delta E_V$  falls within the range of 0.75–1 eV, while conduction band offset  $\Delta E_C$  is within the range of 0.2–0.4 eV [3–5]. These values are optimum for a *n*-GaP/*p*-Si heterojunction. A large  $\Delta E_V$  value forms a high potential barrier that inhibits the transport of minority carriers (holes) from *p*-Si to *n*-GaP and their subsequent recombination at surface states. At the same time, low  $\Delta E_C$  contributes to the formation of a low potential barrier, ensuring unhindered transport of majority carriers (electrons). Solar cells based on anisotype *n*-GaP/*p*-Si heterojunctions demonstrated the possibility of expanding the photosensitivity spectrum in

the short-wave region [6]. It should be noted that thin-film technology with plasma deposition holds a special place among the known methods for fabrication of GaP/Si heterostructures for solar cells, since it has the greatest potential for large-scale production [7,8]. However, almost no reliable experimental data on the electronic properties of the heterojunction between wider-bandgap AlP (2.5 eV) and Si are available at present. A theoretical estimate of  $\Delta E_V = 0.88$ –1 eV may be obtained by analyzing literature data [9,10]. Experimental studies have been performed only for GaP/AlP heterojunctions ( $\Delta E_V = 0.62$  eV) [11]. Using the obtained data, one may evaluate the electron affinity of AlP and find a rough estimate of  $\Delta E_V$  at the AlP/Si interface, which also turns out to be close to 1 eV. Anisotype heterojunction *n*-AlP/*p*-Si with  $\Delta E_V = 1$  eV (Fig. 1, *a*) may be an effective selective contact for electrons, which is of potential interest for solar cell engineering. Experimental studies of the electronic properties of AlP/Si heterojunctions need to be performed to confirm this assumption.

In the present study, AlP/Si heterostructures have been formed for the first time by combined plasma-enhanced and atomic layer deposition, and their electronic properties were examined. AlP layers were deposited onto substrates made of fused quartz and single-crystal (100) *n*- and *p*-type Si with phosphorus and boron concentrations of  $10^{15}$  cm<sup>-3</sup>, respectively. Immediately prior to deposition, Si substrates were treated with a 10% HF/H<sub>2</sub>O solution to remove natural oxide and ensure hydrogen passivation. An Oxford Plasmalab System 100 PECVD setup was used to perform deposition at a temperature of 380°C and a pressure of 350 mTorr. Layer-by-layer growth was achieved by implementing the following cycle: decompo-

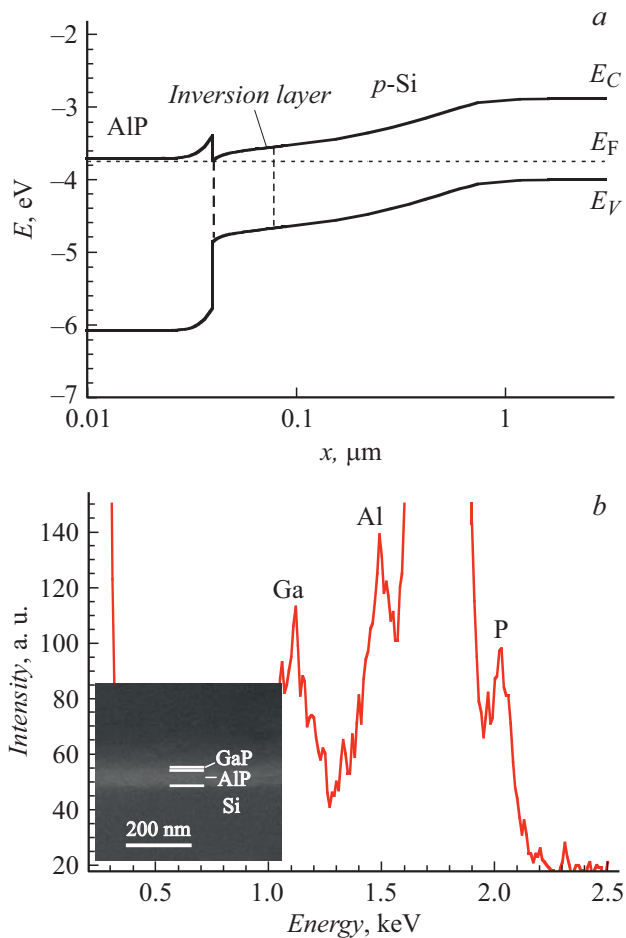


**Figure 1.** *a* — Band diagram of the  $n$ -AIP/ $p$ -Si heterojunction for  $\Delta E_C = 0.35$  eV. *b* — Energy-dispersive spectrum and SEM image (isometric view at an angle of  $20^\circ$ ) of the GaP/AIP structure on Si.

sition of phosphine ( $\text{PH}_3$ ) in plasma of a radio-frequency (13.56 MHz) discharge with a power density of  $90 \text{ mW/cm}^2$ ; purging with Ar; thermally activated surface reaction of trimethylaluminum; purging with Ar. Plasma was ignited only at the stage of phosphorus deposition. The approximate thickness of an AIP layer formed in the above cycle is 0.1 nm. The total AIP layer thickness is 40 nm. To ensure AIP stability in air, a 5-nm-thick GaP layer was deposited on top of the AIP layer in the same process using a similar technique and mode of deposition [8]. The only difference was the use of trimethylgallium as a source of group III element in the deposition of GaP.

The examination of structure and surface morphology of layers with a SUPRA 25 (Carl Zeiss) scanning electron microscope (SEM) revealed that AIP/GaP layers on Si have a smooth surface and a uniform structure (see the inset in Fig. 1). The optical transmittance and reflectance spectra measured for layers deposited onto a quartz substrate demonstrated their high optical transparency within the  $0.4\text{--}1.1 \mu\text{m}$  range and provided an opportunity to estimate the band gap ( $\sim 2.5 \text{ eV}$ ). The composition of the

obtained AIP layers was verified in energy-dispersive X-ray spectroscopy experiments performed with an Oxford Instruments Ultim detector attached to the electron microscope. The spectrum presented in Fig. 1, *b* contains peaks at 1.486 and 2.013 keV, which correspond to  $K_\alpha$  characteristic emission lines of Al and P, respectively, and a peak at 1.098 keV corresponding to the  $L_\alpha$  line of Ga. Quantitative estimates indicate that the composition of AIP and GaP layers is near-stoichiometric (within the limits of error associated with their small thickness).

Ohmic In contacts were formed to GaP/AIP structures on  $n$ - and  $p$ -type Si substrates. The current–voltage curves (CVCs) measured in the dark at 300 K are ohmic in nature (linear) for structures formed on  $n$ -Si and rectifying for structures on  $p$ -Si (Fig. 2). This CVC behavior suggests that AIP layers feature  $n$ -type conductivity. These results agree with those obtained earlier for GaP/Si heterostructures fabricated by the same method in [12], where silicon was incorporated from the substrate into GaP layers in the process of deposition. The linear CVC shape is also indicative of unimpeded carrier transport through the GaP/AIP heterointerface. GaP/AIP structures on  $p$ -Si exhibit photovoltaic properties under illumination (Fig. 2). When the measurement temperature went down, the idle voltage grew, while the short-circuit current decreased. These changes are typical of silicon photovoltaic converters. It should be noted that the CVC retains a shape characteristic of solar cells with no kinks at temperatures up to 100 K. This lack of kinks under illumination at low temperatures is indicative of unimpeded transport of electrons across the AIP/Si interface from  $p$ -Si to AIP. Therefore, the potential barrier at the AIP/Si interface formed by  $\Delta E_C$  either has a small height ( $\Delta E_C \leq 0.4 \text{ eV}$ ) or is transparent to tunneling due to the very high level of AIP doping. The low conductivity of AIP layers grown on a quartz substrate makes it difficult to measure their doping level. However, similar to  $n$ -GaP/ $p$ -Si examined earlier in [12], structures grown on  $p$ -Si have a fairly high surface conductivity, which is attributable to an inversion layer with a surface electron concentration of  $\sim 1.7 \cdot 10^{12} \text{ cm}^{-2}$  and an electron mobility of  $\sim 180 \text{ cm}^2 \cdot \text{V}^{-1} \cdot \text{s}^{-1}$  that were determined using the Hall method. Conductivity type inversion occurs in the near-surface region of Si due to strong band bending at the AIP/Si interface (Fig. 1, *a*), which is governed by the level of  $n$ -AIP doping and the  $\Delta E_C$  value. If the levels of  $n$ -AIP and  $p$ -Si doping and the surface electron concentration ( $n_s$ ) are known, one may obtain a numerical estimate of  $\Delta E_C$ . Specifically, if the level of  $n$ -AIP doping is  $10^{18} \text{ cm}^{-3}$ , the measured  $n_s$  value corresponds to  $\Delta E_C \sim 0.35 \text{ eV}$ .

Additional  $C$ – $V$  profiling measurements [13] were performed in order to estimate the distribution of carrier concentration at the AIP/Si interface. A Schottky barrier was formed for this purpose by vacuum deposition of Au on the surface of GaP/AIP structures grown on  $n$ -Si, and an ohmic In contact was formed on the back side. The CVC of produced structures is rectifying in nature, which verifies the formation of a Schottky barrier; at the same

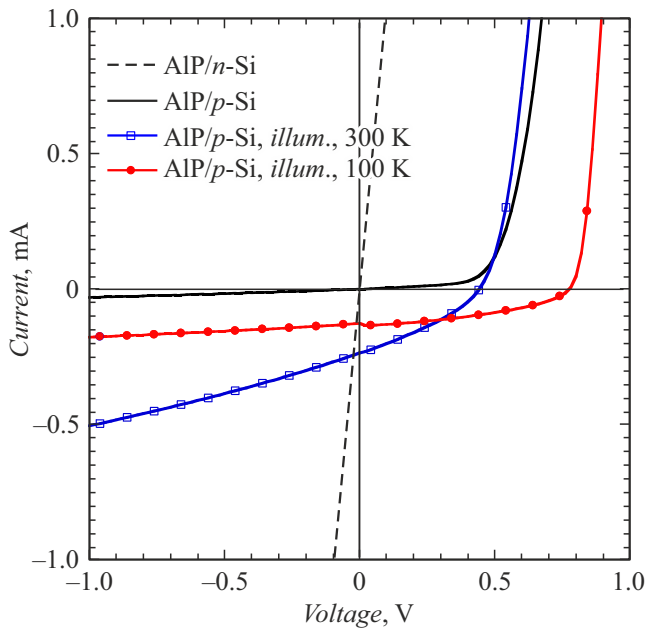


**Figure 2.** CVCs for GaP/AIP on *n*-Si and *p*-Si with In contacts in the dark and for GaP/AIP on *p*-Si under illumination at a temperature of 300 and 100 K.

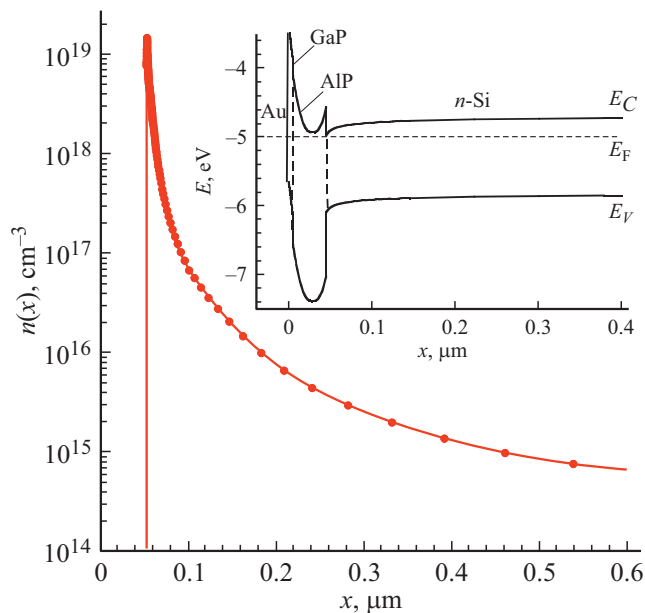


**Figure 3.** Band diagram of GaP/AIP on *n*-Si with an upper Schottky barrier (inset) and electron concentration distribution profile  $n(x)$  obtained by measuring the  $C-V$  characteristics of this structure.

time, an increase in leakage currents under reverse voltage was observed. To reduce the influence of reverse currents,  $C-V$  measurements were performed at a temperature of 180 K and a frequency of 1 MHz with the use of a nitrogen cryostat and an E4980A-001 Keysight *LCR* meter. Figure 3 presents electron concentration distribution profile  $n(x)$  for

AIP/Si calculated based on the  $C-V$  measurement data in accordance with the procedure specified in [13]. The obtained  $n(x)$  dependence features a carrier concentration peak at a depth of  $\sim 50$  nm, which corresponds to the AIP/*n*-Si heterointerface. This is indicative of accumulation of electrons in the near-surface region of *n*-Si due to band bending induced by  $\Delta E_C$  (see the inset in Fig. 3). The electron concentration decreases with profiling depth and corresponds to the level of *n*-Si substrate doping ( $\sim 10^{15} \text{ cm}^{-3}$ ) at  $x > 0.5 \mu\text{m}$ . Since the width of the space charge region formed by the Schottky barrier turned out to be comparable to the AIP layer thickness, the measured  $n(x)$  profile does not provide information on the AIP doping level. However, the obtained results of numerical calculation of  $n(x)$  profiles for various AIP doping levels  $N_d^{\text{AIP}}$  and  $\Delta E_C$  values make it possible to perform a quantitative assessment. At  $N_d^{\text{AIP}} \geq 5 \cdot 10^{18} \text{ cm}^{-3}$ , the space charge region width (20 nm) becomes significantly lower than the AIP layer thickness (40 nm). The  $N_d^{\text{AIP}}$  value should then be reflected in the resulting  $n(x)$  profile at minimum applied voltages. At the same time, the AIP layer becomes completely depleted at  $N_d^{\text{AIP}} \leq 1 \cdot 10^{18} \text{ cm}^{-3}$ , and band bending in the near-surface region of *n*-Si leads, even at very high  $\Delta E_C$  values (up to 1 eV), to the accumulation of electrons with a concentration an order of magnitude lower than the measured value. Thus, having analyzed the experimental  $n(x)$  profile, we determined the range of  $N_d^{\text{AIP}} (1-5) \cdot 10^{18} \text{ cm}^{-3}$  that corresponds to estimated  $\Delta E_C$  values of  $0.35 \pm 0.10 \text{ eV}$ . These  $\Delta E_C$  values agree well with the results of measurements of the electron concentration in the inversion layer for AIP/*p*-Si structures. However, it should be noted that both estimates were based on a calculation that did not take into account the potential pinning of the Fermi level at the AIP/Si interface. At the same time, the obtained values of  $\Delta E_C$  agree closely with theoretical estimates of the band offset for the AIP/Si interface [9,10]. Most importantly, the obtained range of relatively small  $\Delta E_C$  is also in agreement with the results of measurement of AIP/*p*-Si CVCs under illumination at low temperature. Thus, it was demonstrated experimentally that  $\Delta E_C$  at the AIP/Si interface is significantly lower than  $\Delta E_V$  and, consequently, AIP layers may be used as an effective electron-selective contact to Si.

## Funding

This study was supported by a grant from the Russian Science Foundation, project № 21-79-10413 (<https://rscf.ru/project/21-79-10413/>).

## Conflict of interest

The authors declare that they have no conflict of interest.

## References

- [1] M.A. Green, E.D. Dunlop, G. Siefer, M. Yoshita, N. Kopidakis, K. Bothe, X. Hao, Prog. Photovolt. Res. Appl., **31**, 3 (2023). DOI: 10.1002/pip.3646
- [2] J. Bullock, M. Hettick, J. Geissbühler, A.J. Ong, T. Allen, C.M. Sutter-Fella, T. Chen, H. Ota, E.W. Schaler, S. De Wolf, C. Ballif, A. Cuevas, A. Javey, Nat. Energy, **1**, 15031 (2016). DOI: 10.1038/nenergy.2015.31
- [3] I. Sakata, H. Kawanami, Appl. Phys. Express, **1**, 091201 (2008). DOI: 10.1143/APEX.1.091201
- [4] P. Perfetti, F. Patella, F. Sette, C. Quaresima, C. Capasso, A. Savoia, G. Margaritondo, Phys. Rev. B, **30**, 4533 (1984). DOI: 10.1103/PhysRevB.30.4533
- [5] A.D. Katnani, G. Margaritondo, Phys. Rev. B, **28**, 1944 (1983). DOI: 10.1103/PhysRevB.28.1944
- [6] H. Wagner, T. Ohrdes, A. Dastgheib-Shirazi, B. Puthen-Veettil, D. König, P.P. Altermatt, J. Appl. Phys., **115**, 044508 (2014). DOI: 10.1063/1.4863464
- [7] S. Yun, Ch.-H. Kuo, P.-Ch. Lee, S.T. Ueda, V. Wang, H. Kashyap, A.J. Mcleod, Z. Zhang, Ch.H. Winter, A.C. Kummel, Appl. Surf. Sci., **619**, 156727 (2023). DOI: 10.1016/j.apsusc.2023.156727
- [8] A.V. Uvarov, A.S. Gudovskikh, V.N. Nevedomskiy, A.I. Baranov, D.A. Kudryashov, I.A. Morozov, J.-P. Kleider, J. Phys. D: Appl. Phys., **53**, 345105 (2020). DOI: 10.1088/1361-6463/ab8bfd
- [9] N.E. Christensen, Phys. Rev. B, **37**, 4528 (1988). DOI: 10.1103/PhysRevB.37.4528
- [10] Y. Hu, C. Qiu, T. Shen, K. Yang, H. Deng, J. Semicond., **42**, 112102 (2021). DOI: 10.1088/1674-4926/42/11/112102
- [11] S. Nagao, T. Fujimori, H. Gotoh, H. Fukushima, T. Takano, H. Ito, S. Koshihara, F. Minami, J. Appl. Phys., **81**, 1417 (1997). DOI: 10.1002/(SICI)1521-3951(199901)211:1;63::AID-PSSB63;3.0.CO;2-G
- [12] A.S. Gudovskikh, A.V. Uvarov, I.A. Morozov, A.I. Baranov, D.A. Kudryashov, E.V. Nikitina, A.A. Bukatin, K.S. Zelentsov, I.S. Mukhin, A. Levchenko, S. Le Gall, J.-P. Kleider, J. Renew. Sustain. Energy, **10**, 021001 (2018). DOI: 10.1063/1.5000256
- [13] S.R. Forrest, in: *Heterojunction band discontinuities: physics and device applications* (Elsevier, 1987), p. 311.

*Translated by D.Safin*